Comparison of Chemical and Interpretative Methods: the Carbon- Boron π-Bond as a Test Case

Radhika Gupta, Elixabete Rezabal, Golshid Hasrack, Gilles Frison

Comparison of Chemical and Interpretative Methods: the Carbon-Boron π-Bond as a Test Case

Radhika Gupta,[a] Elixabete Rezabal,[a,b] Golshid Hasrack,[a] Gilles Frison*[,a]

[a] LCM, CNRS, Ecole polytechnique, Institut Polytechnique de Paris, 91128 Palaiseau, France
[b] Faculty of Chemistry, University of the Basque Country UPV/EHU, Donostia International Physics Center (DIPC), 20018 Donostia, Spain

Abstract

Quantum chemical calculations and NBO, ETS-NOCV, QTAIM and ELF interpretative approaches have been carried out on C-donor ligand-stabilized dihydrido borenium cations. Numerous descriptors of the C-B π-bond strength obtained from orbital localization, energy partitioning or topological methods as well as from structural and chemical parameters have been calculated for 39 C-donor ligands including N-heterocyclic carbenes and carbones. Comparison of the results allows the identification of *relative* and *absolute* descriptors of the π interaction. For both families of descriptors excellent correlations are obtained. This enables the establishment of a π-donation capability scale and shows that the interpretative methods, despite their conceptual differences, describe the same chemical properties. These results also reveal noticeable shortcomings in these popular methods, and some precautions that need to be taken to interpret their results adequately.

Introduction

Chemical bonds, among other "fuzzy" chemical concepts,[1,2] are not univocally defined and their quantification is not straightforward because they are not a quantum mechanical observable. However, chemical bonding is a key concept in chemistry, a cornerstone of this science.[3,4] In that context, numerous approaches have been developed in order to describe, classify and measure chemical bond. Experimentally, it is difficult to quantify a chemical bond, even if widely known indicators exist. The bond length, which from the chemist's point of view should be approximately correlated to its strength, can indeed be empirically related to a bond index[5] or compared to the sum of the covalent radii of the atoms involved.[6] The activation barrier associated to the rotation around the bond allows to differentiate a single bond (free rotation) from a double bond (strong rotation barrier).

The advent of theoretical and computational chemistry has made it possible to have straightforward access to these parameters by calculation, and simultaneously has led to the development of methods for bond analysis. These methods use different approaches to describe the molecular system under study.[7] A first representation can be made from the molecular orbitals used to describe the wave function. The bond order for π-bond in the Hückel framework defined by Coulson,[8] the Wiberg Bond Index (WBI)[9] and the Mayer bond order[10] are prominent examples derived from this approach.[11] Bonding analysis can also result from different procedures leading to localized molecular orbitals[12-14] or natural orbitals,[15] leading to methods such as the Localized orbital bonding analysis (LOBA) method[16,17] and the well-known natural bonding orbital (NBO) method.[18]

A second group of methods is based on the real-space partition of the molecular space using various functions such as the electronic density, the Pauli kinetic energy density, the reduced density gradient or the single-Exponential decay detector. These functions are used in the Bader's Quantum theory of atoms in molecules (QTAIM) method,[19] the electron localization function (ELF) method,[20,21] the non-covalent interaction (NCI) index[22] and the density overlap regions indicator (DORI) analysis,[23] respectively. An interesting picture of the chemical bond can also be obtained through the variations in isotropic magnetic shielding around a molecule,[24] or with the charge displacement analysis method.[25]

Chemical bond analysis can also be performed using energy decomposition approaches, such as the symmetry-adapted perturbation theory (SAPT) scheme,[26] the extended transition state (ETS)[27,28] or the energy decomposition analysis (EDA)[29] methods, the latter being possibly combined with the natural orbitals for chemical valence (NOCV) theory.[30]

Finally, although force constants are known not to properly match the bond strengths,[31] derived methods such as the concept of adiabatic internal vibrational modes,[32] or the local stretching force[33] and compliance constants[34] also provide noteworthy chemical bond descriptors.

These many interpretative methods are widely used in the literature to provide insights into the nature of chemical bonds.[35-43] However, this plethora of methods, while of value in providing complementary visions of the same subject,[44-46] is also troublesome, in the sense that contradictory descriptions can result, leading to many controversies in the literature, whether it is to describe for example alkaline earth-[47-49] or metal-ligand bonds,[50,51] multiple bonds[52-54] weak bonds,[55-61] or rotational barrier of single bond.[62,63] In many cases too, there is no significant discrepancy between two different approaches, but the agreement between the calculated parameters that are supposed to describe the same chemical property using different methods is far from perfect. A noteworthy

example is given in a recent study in which the internal π-donation to the carbene center within 15 *N*-heterocyclic carbenes (NHC) has been estimated through NBO and ETS-NOCV approaches.[64] Despite the relevance of the two selected descriptors, the coefficient of determination (R^2) is not more than 0.89. If such computational approach is a powerful tool to qualitatively predict the trend comparing chemically similar systems, it raises questions about the reasons for the observed differences.

Depending on the theoretical model used, the numerical differences between several bond descriptors may result from many factors, such as the comparison of descriptors which might not be related to the same chemical concept, the misuse of methods, the misinterpretation of the results or the existence of conceptual problems in the definition of the descriptors. It is currently difficult to distinguish between these different assumptions and opinions may differ,[65,66] even if numerous efforts have been made to compare various methods, to analyze their differences and to propose unified approaches.[67-70]

The ability to establish cross correlations (or lack of correlations) between different approaches would, however, provide a better knowledge of the nature of the calculated descriptors, of the chemical concept under investigation, and could help in the development of future interpretative methods. In this context, the focus of the present work lies on the modeling, through various theoretical approaches, of the π-interaction between neutral divalent carbon-donor compounds and cationic BH_2^+ moiety. Borenium cations R_2BL^+ are well-known boron Lewis acids.[71] These boron species have been used in numerous catalytic processes.[72-75] They are stabilized through electronic π-donation from the π-cloud of the boron substituents,[76-79] and neutral divalent carbon-donor compounds, such as normal NHC,[80-85] mesoionic NHC[86] and carbones,[87] have been used for this purpose (Scheme 1). For dihydrido borenium (R = H), only their two-electrons σ-donor L ligand provide partial mitigation of their electron deficiency and their stabilization requires strong π-donor.[88,89] DFT studies on C-donor ligand-BR_2^+ borenium reveal a short CB bond reflecting a partial double-bond character due to C→B π-electronic transfer.[82,84,87-91] Beyond structural parameters, various theoretical indicators have been used to analyze the electronic structure of these and other related compounds,[92-94] among them the nature of the highest occupied and lowest unoccupied molecular orbitals (HOMO/LUMO), the atomic charges, the energy associated to the σ- and π-donation through energy decomposition analysis of the B-C bond, and the Wiberg bond index between these two atoms. Only few studies have used such indicators to compare the bonding situation in borenium complexes. The comparison of the bonding in various complexes between carbones $(PPh_3)_2C$ and EH_2^q (E^q = Be, B^+, C^{2+}, N^{3+}, O^{4+}) has been performed with the ETS-NOCV approach.[90] Recently, a combination of energy decomposition analysis methods has been used to clarify the theoretical measurement of the π-interactions strength within main group-NHC complexes, including NHC-borenium complexes. [95] Based on these previous studies, C-donor ligand - dihydrido borenium complexes, in which the π-interaction between the two fragments is limited to the C→B π-donation, appear as ideal models to assess the relevance of π-bond descriptors.

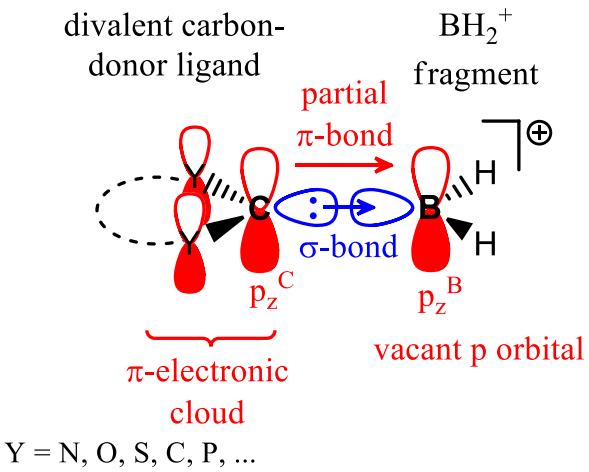

Scheme 1. Schematic description of the orbital-based σ- (blue) and π- (red) interactions in neutral divalent carbon-donor – BH_2^+ (**X**$^{//}$-BH_2^+) complexes

Result and discussion

Geometrical structures

39 divalent carbon compounds, including normal NHC (**1**-**2**, **4**, **6**, **8**, **10**, **12**, **14**, **16**, **20**-**24**, **26**-**28**, **30**-**33**), mesoionic NHC (**9**, **11**, **13**, **15**, **17**-**19**, **25**, **29**), cyclic alkyl amino carbenes (cAAC **3**, **5**, **7**), carbodiphosphoranes (**35**-**36**) and carbodicarbenes (**34**, **37**-**39**), have been selected, so as to ensure a wide variety of geometrical structures and electronic properties (Scheme 2).[96-99] Most of them, but **5**, **7**, **17**, **23**-**24**, **26**-**28** and **32**, are unsubstituted or "parent" molecules, preventing steric interference in the electronic analysis of their BH_2^+ complexes. The divalent carbon atom of **1**-**39** is linked to two atoms, noted Y, and possesses a lone pair located in the Y-C-Y plane. **1**-**39** bind to the BH_2^+ moiety to form the borenium cations **X**-BH_2^+ (**X** = **1**-**39**). Geometry optimization of **X**-BH_2^+ (**X** = **1**-**39**) at the DFT B3LYP/TZVP level (see the Supporting Information for the computational methods) leads to minimum on the potential energy surface for which the BH_2 and Y_2C moiety are coplanar or almost coplanar,[100] except for **3**, **5** and **7** (vide infra). This planar conformation will be noted hereafter as **X**$^{//}$-BH_2^+. In addition to the σ-B-C bond formed by the donation of the in-plane lone pair of the carbon atom to the vacant sp^2-orbital of the boron atom (Scheme 1), this planarity supports the existence of a partial π-bond, the strength of which is supposed to depend on the nature of the π-system of the divalent donor ligand. The **X**$^{//}$-BH_2^+ conformation of **X**-BH_2^+ (**X** = **3**, **5**, **7**) is a transition state for the rotation around the C-B bond, whereas the BH_2 and Y_2C moiety are perpendicular (Y-C-B-H dihedral angle around 90°) in the ground state. This conformation is noted as **X**$^{\perp}$-BH_2^+ in the following. This result suggests weak π-donation capability for **3**, **5** and **7**. Furthermore, in addition to σ- and π-donations, it is likely that there are other weak electronic or steric interactions between the BH_2 and the C-donor ligand in the **X**-BH_2^+ complexes.

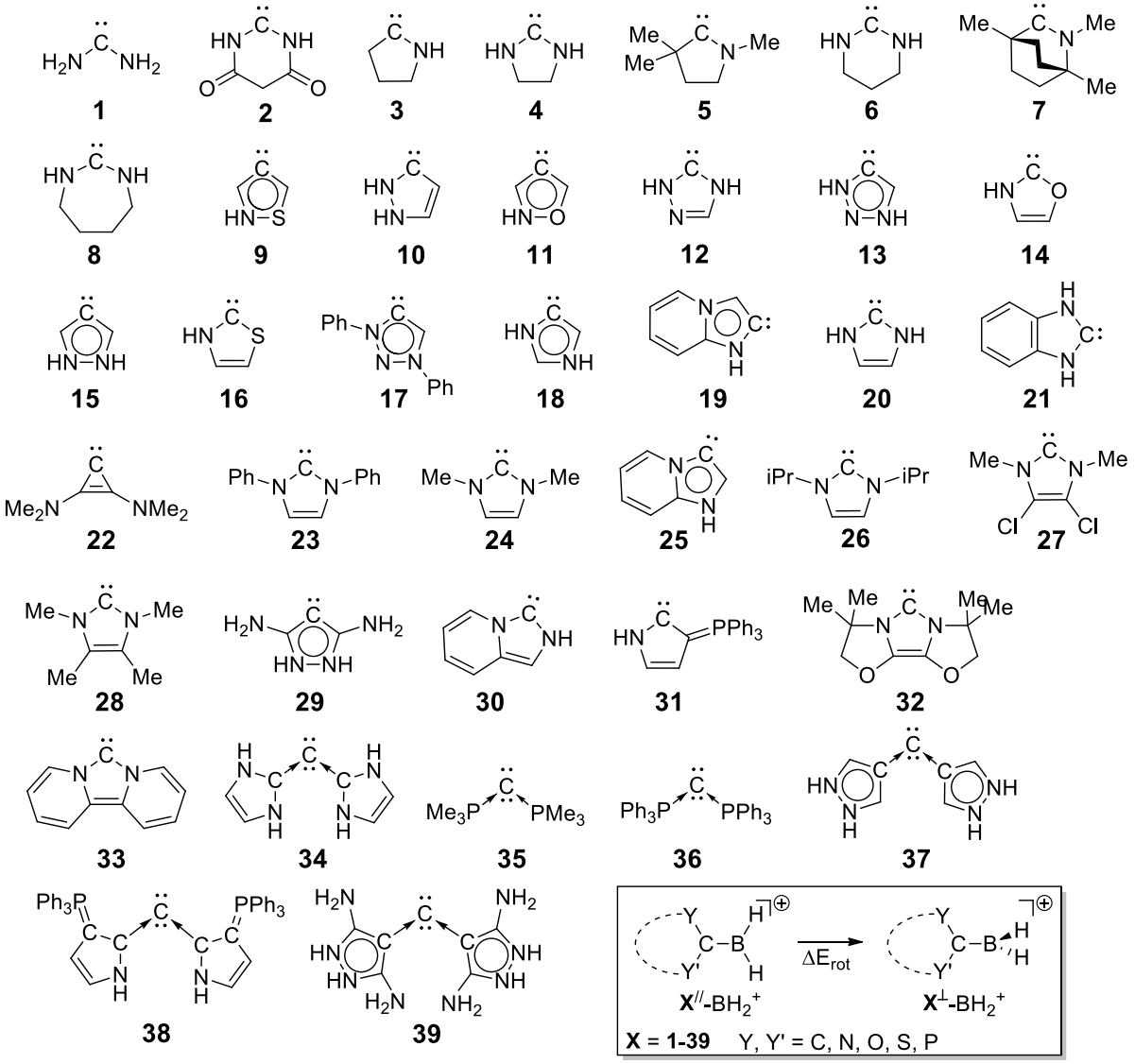

Scheme 2. **X**-BH_2^+ (X = **1**-**39**) borenium cation studied in this work.

π-bonding descriptors based on chemical insight

From the chemist's point of view, a double bond differs from a single bond by several features, in particular a shorter bond length and a significant energy barrier associated with the rotation around the bond. To estimate these characteristics, we calculated the energy barrier ΔE_{rot} associated with the rotation around the C-B bond, i.e. the energy required to go from $\mathbf{X}^{//}$-BH_2^+ to $\mathbf{X}^{\perp}$-BH_2^+ (Scheme 2). In all cases except **3**, **5** and **7**, $\mathbf{X}^{\perp}$-BH_2^+ is a transition state for this rotation and ΔE_{rot} has a positive value which range from 5 kJ/mol for **2** to 172 kJ/mol for **39**. For **3**, **5** and **7**, a negative value is obtained (between -29 and -13 kJ/mol) (see Table S1). This wide range of values confirms the structural diversity of compounds **1**-**39** in terms of π-donation capability. At the same time, the change from $\mathbf{X}^{//}$-BH_2^+ to $\mathbf{X}^{\perp}$-BH_2^+ induces in most cases, except for **1**-**5** and **7**, a slight increase in the B-C bond length, in line with the cancellation of the π-transfer to the vacant p_{vac}^{B} orbital, which is responsible for the partial double bond character.

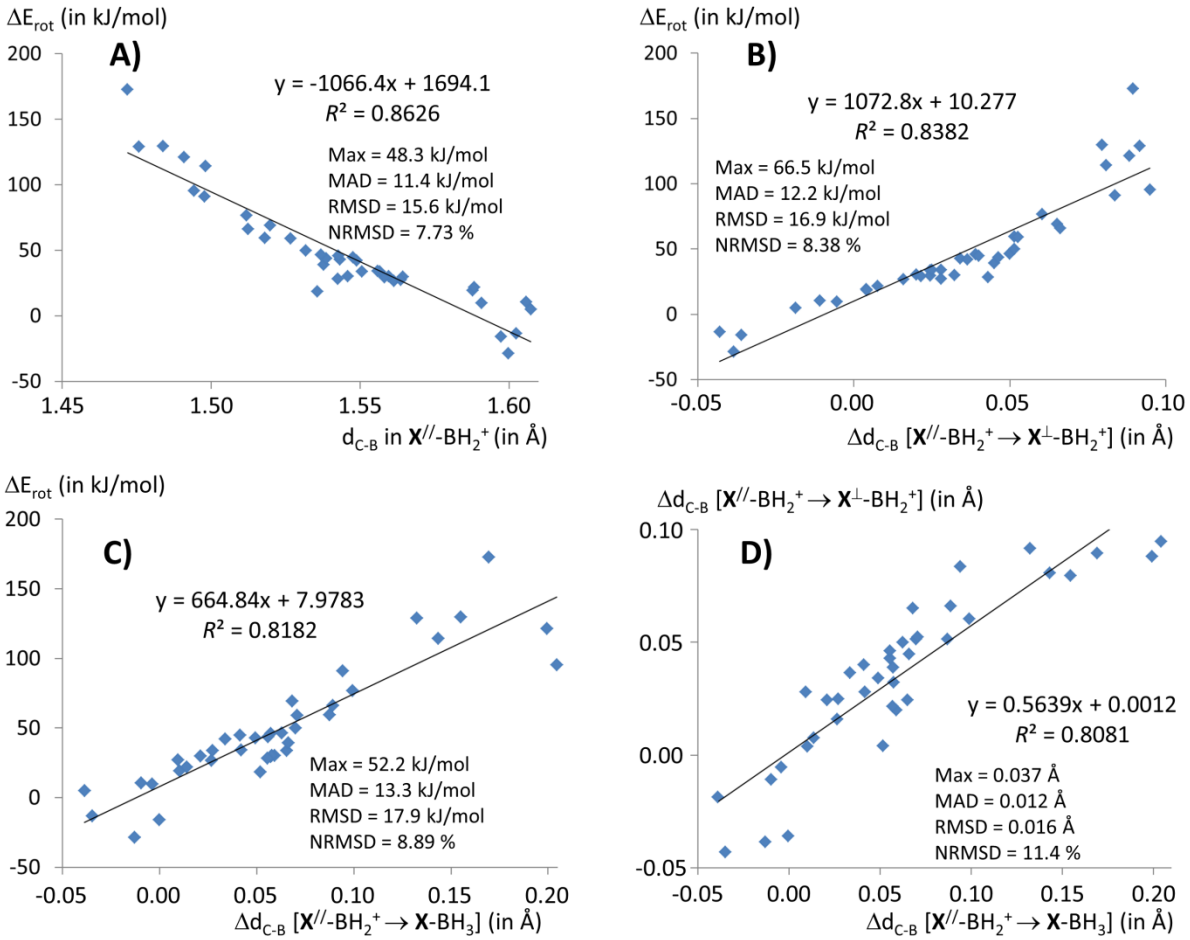

Figure 1. Correlation plots for **X**-BH_2^+ complexes computed at the B3LYP/TZVP level between: the energy barrier ΔE_{rot} associated with the rotation around the C-B bond *vs*. the C-B bond length ($d_{C\text{-}B}$) in $\mathbf{X}^{//}$-BH_2^+ (A); ΔE_{rot} *vs*. the change in the C-B bond length ($\Delta d_{C\text{-}B}$) when going from $\mathbf{X}^{//}$-BH_2^+ to $\mathbf{X}^{\perp}$-BH_2^+ (B) and **X**-BH_3 (C); $\Delta d_{C\text{-}B}$ when going from $\mathbf{X}^{//}$-BH_2^+ to $\mathbf{X}^{\perp}$-BH_2^+ *vs.* to **X**-BH_3 (D). Linear regression equation, coefficients of determination (R^2), maximum absolute deviations (Max), mean absolute deviations (MAD), root mean square deviations (RMSD) and normalized RMSD (NRMSD) are reported.

In agreement with the chemical expectation, Figure 1A indicates that there is a rough match between the C-B bond length ($d_{C\text{-}B}$) in $\mathbf{X}^{//}$-BH_2^+ and the energy barrier ΔE_{rot} associated with the rotation around the C-B bond. This correlation is only fairly good (R^2 = 0.86), indicating that these descriptors do not measure exactly the same chemical property. This discrepancy may be due to the fact that $d_{C\text{-}B}$ includes both the σ- and the π-interactions whereas ΔE_{rot} characterizes only the latter and measure an evolution from $\mathbf{X}^{//}$-BH_2^+ to $\mathbf{X}^{\perp}$-BH_2^+. In order to mitigate these differences, the C-B bond elongation $\Delta d_{C\text{-}B}$ during the rotation of the BH_2 group has been considered (Figure 1B). A correlation is again obtained, but it is not better than the one observed previously (R^2 = 0.84). A similar correlation (R^2 = 0.82, Figure 1C) is obtained by considering the C-B bond elongation when the H^- anion is added to $\mathbf{X}^{//}$-BH_2^+ to form the donor-acceptor **X**-BH_3 complex. The larger C-B bond length in **X**-BH_3 compared to $\mathbf{X}^{\perp}$-BH_2^+, as well as the moderately good correlation between $\Delta d_{C\text{-}B}$ to reach these two complexes from $\mathbf{X}^{//}$-BH_2^+ (R^2 = 0.81, Figure 1D), indicate that these two ways of considering a purely σ-bond are not equivalent. It is likely that the interaction between **X** and the rotated BH_2^+ or BH_3 groups in these complexes is not only a σ-interaction, but also includes other component such as an electronic transfer from the **X** σ-system to the vacant p-orbital of the rotated

BH_2^+ group in $\mathbf{X}^{\perp}$-BH_2^+ (*vide infra*). This first approach therefore does not provide an unbiased measure of the π-donation capability of **X**.

π-bonding descriptors based on the NBO approach

In the framework of the NBO analysis, the C→B π-donation in $\mathbf{X}^{//}$-BH_2^+ complexes can be characterized through several indicators. First, we compute the WBI which is known to have good agreement with empirical bond order. Values of WBI between 0.83 ($\mathbf{2}^{//}$-BH_2^+) and 1.43 ($\mathbf{39}^{//}$-BH_2^+) have been obtained (Table S2). Comparisons between WBI and the C-B bond length show similar trend, but with moderate correlation (R^2 = 0.82. Figure S1). A better correlation is observed between WBI($\mathbf{X}^{//}$-BH_2^+) and ΔE_{rot} (R^2 = 0.90, Figure 2A). For $\mathbf{X}^{\perp}$-BH_2^+ complexes for which approximately a single C-B bond is expected, the WBI ranges as anticipated from 0.84 to 0.92. A revised π-bond order can be estimated by calculating the difference between the WBI obtained for $\mathbf{X}^{//}$-BH_2^+ and $\mathbf{X}^{\perp}$-BH_2^+ (ΔWBI).[101] ΔWBI lies between -0.06 and 0.50, which confirms the diverse π-donation capability of **1**-**39**. Small negative values are obtained for **3**, **5** and **7** for which the "perpendicular" conformer is more stable than the planar one. The ΔWBI parameter, which accounts for both the interaction in $\mathbf{X}^{//}$-BH_2^+ and $\mathbf{X}^{\perp}$-BH_2^+ complexes, as is the case with ΔE_{rot}, leads as expected to an improved but still imperfect correlation (R^2 = 0.92, Figure 2B).

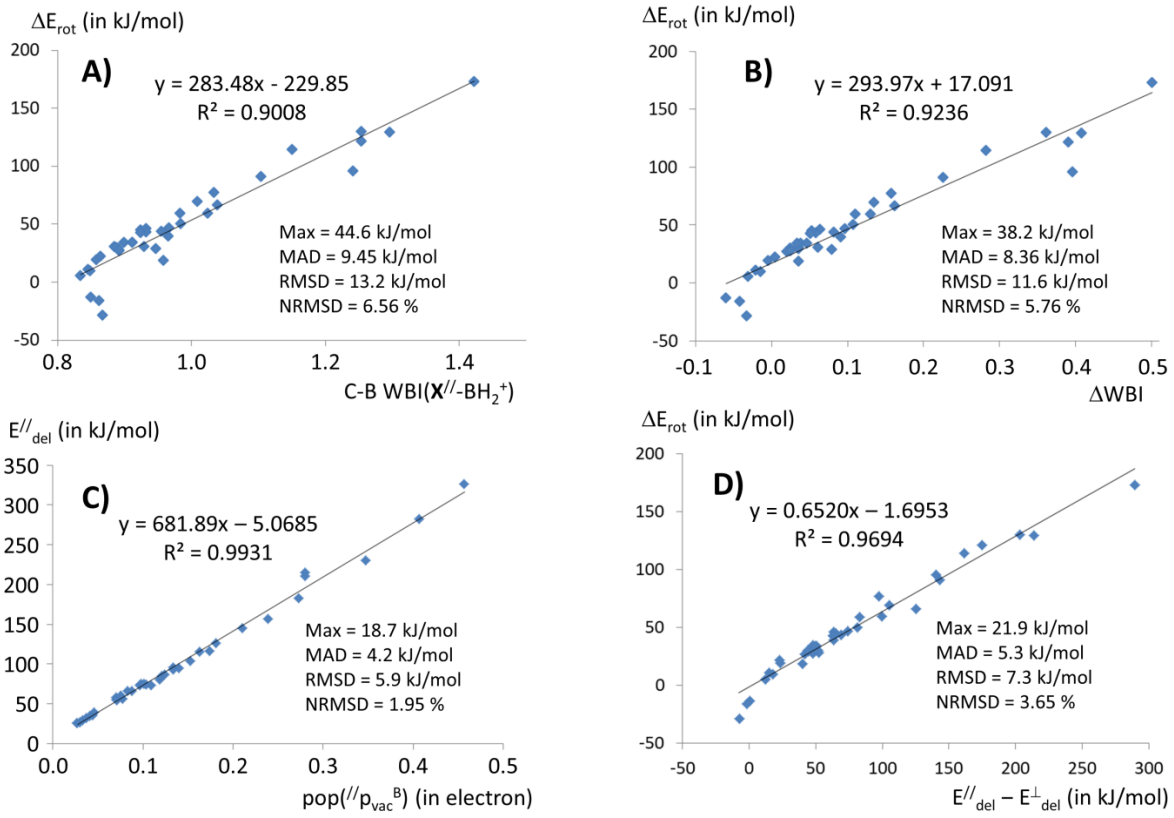

Figure 2. Correlation plots for **X**-BH_2^+ complexes computed at the B3LYP/TZVP level between various descriptors obtained with the NBO method.

WBI has been originally built as a quantitative measure of the electronic population occupying bonding molecular orbital.[9] Similarly, the electronic population of the p_{vac}^B orbital,[96,102] noted as pop($^{//}p_{vac}^B$), is expected to measure the π-donation strength from **X** to BH_2^+ in $\mathbf{X}^{//}$-BH_2^+ complexes. Indeed, by construction, the p_{vac}^B orbital is utterly empty for the BH_2^+ fragment alone, whereas in the $\mathbf{X}^{//}$-BH_2^+ conformation, its population can only come from the π-type orbitals of the **X** moiety.

Pop($^{//}p_{vac}^{B}$) values range from 0.027 to 0.457 electron (see Table S2), again illustrating the diversity of π-donation properties of ligands **1**-**39**. The NBO6 program includes a module that allows to remove specific electronic interactions and to measure their energy contribution (see Computational Methods for details). This "deletion" energy, noted $E^{//}_{del}$, has also been computed for the $\mathbf{X}^{//}$-BH_2^+ conformer by removing the p_{vac}^{B} orbital, thus cancelling any possibility of π-electronic donation from **X** to BH_2^+. It is noteworthy that pop($^{//}p_{vac}^{B}$) and $E^{//}_{del}$ correlate almost perfectly with each other (R^2 = 0.99, Figure 2C). These NBO electronic population and energetic parameters therefore measure the same chemical property. By construction of these descriptors, we assume that they measure the *intrinsic* strength of the π-interaction. Even if they seem to reliably quantify the π-donation capability of the divalent C-donor ligand, showing as expected a significantly higher π-donation for carbones compared to most *N*-heterocyclic carbenes, at this stage, it is not possible to guarantee that these NBO-based indicators are reference data for intrinsic π-bond strengths. This outstanding linear correlation is nevertheless expected to be restrained to bonds between two defined atoms, here boron and carbon atoms, and probably cannot be extended to all bonds (see Computational Methods in the SI). To a lesser extent, the WBI allows also a suitable quantification of the *intrinsic* π-bond, as very good correlation between the C-B bond WBI and either pop($^{//}p_{vac}^{B}$) or $E^{//}_{del}$ is observed ($R^2 > 0.975$, Figure S2).

The above parameters calculated with the NBO method do not correlate satisfactorily with the previously calculated descriptors based on chemical insight. Indeed, an R^2 value of 0.91 is obtained when comparing ΔE_{rot} and pop($^{//}p_{vac}^{B}$) or $E^{//}_{del}$ (Figure S2). This reveals the conceptual difference between the *intrinsic* and the *relative* strength of the π-interaction. The latter, measured by ΔE_{rot}, results from the energy difference between the planar ($\mathbf{X}^{//}$-BH_2^+) and the perpendicular ($\mathbf{X}^{\perp}$-BH_2^+) conformations. To confirm this assumption, the $\mathbf{X}^{\perp}$-BH_2^+ conformers have been used to compute the pop($^{\perp}p_{vac}^{B}$) and $E^{\perp}_{del}$ values (Table S3). In the $\mathbf{X}^{\perp}$-BH_2^+ conformation, the p_{vac}^{B} orbital is coplanar with the **X** moiety and perpendicular to the B-C bond, inducing non-zero overlap between this p orbital and the σ backbone of **X**. The pop($^{\perp}p_{vac}^{B}$) values, which range between 0.006 and 0.071 electron, reveals weak in-plane π-type electronic donation from **X** to p_{vac}^{B}, in agreement with our previous assessment. The deletion of this p orbital leads to $E^{\perp}_{del}$ which nicely correlate with pop($^{\perp}p_{vac}^{B}$) (R^2 = 0.94, Figure S3). Assuming that the interactions between the B-H bonds and the σ-system of **X** in $\mathbf{X}^{//}$-BH_2^+ and those between the B-H bonds and the π-system of **X** in $\mathbf{X}^{\perp}$-BH_2^+ are weak (or similar), and that the B-C σ-bond strength is weakly affected by the rotation of the BH_2 group, ΔE_{rot} is expected to be equivalent to the difference between $E^{//}_{del}$ and $E^{\perp}_{del}$. This is nicely confirmed by the very good correlation obtained between ΔE_{rot} and ($E^{//}_{del} - E^{\perp}_{del}$) ($R^2$ = 0.97, Figure 2D). The descriptors $\Delta E_{del} = E^{//}_{del} - E^{\perp}_{del}$ and $\Delta pop(p_{vac}^{B}) = pop(^{//}p_{vac}^{B}) - pop(^{\perp}p_{vac}^{B})$ are therefore reliable measures of the *relative* strength of the π-interaction, whose reference is ΔE_{rot} (see also Figure S3). This also supports our hypothesis that $E^{//}_{del}$ and pop($^{//}p_{vac}^{B}$) are good descriptors of the intrinsic π-bond strength. It should be noted that the absolute values of ΔE_{rot} and ΔE_{del} are different, the former being significantly lower than the latter. Features of the NBO approach, which allows only bonding interactions to be calculated and does not cover antibonding contributions,[103] explains the systematic overestimation of ΔE_{del} (*vide infra*).

π-bonding descriptors based on the ETS-NOCV approach

The ETS-NOCV method allows to calculate the energy and to identify the nature of the different orbital interactions between two fragments. Diagonalization of the deformation density matrix due to bonding provides eigenvectors named natural orbitals for chemical valence (NOCVs). Pairs of NOCV, having opposite eigenvalues υ_i and $-\upsilon_i$ and for which an energy ΔE_i is associated, are

obtained. They enable to visualize the deformation of the density associated with each interaction and to determine its nature. Therefore, the total orbital interaction between fragments is partitioned into several chemically interpretable interactions ($NOCV_i$) for which energy (ΔE_i) and charge transfer (υ_i) are quantified.

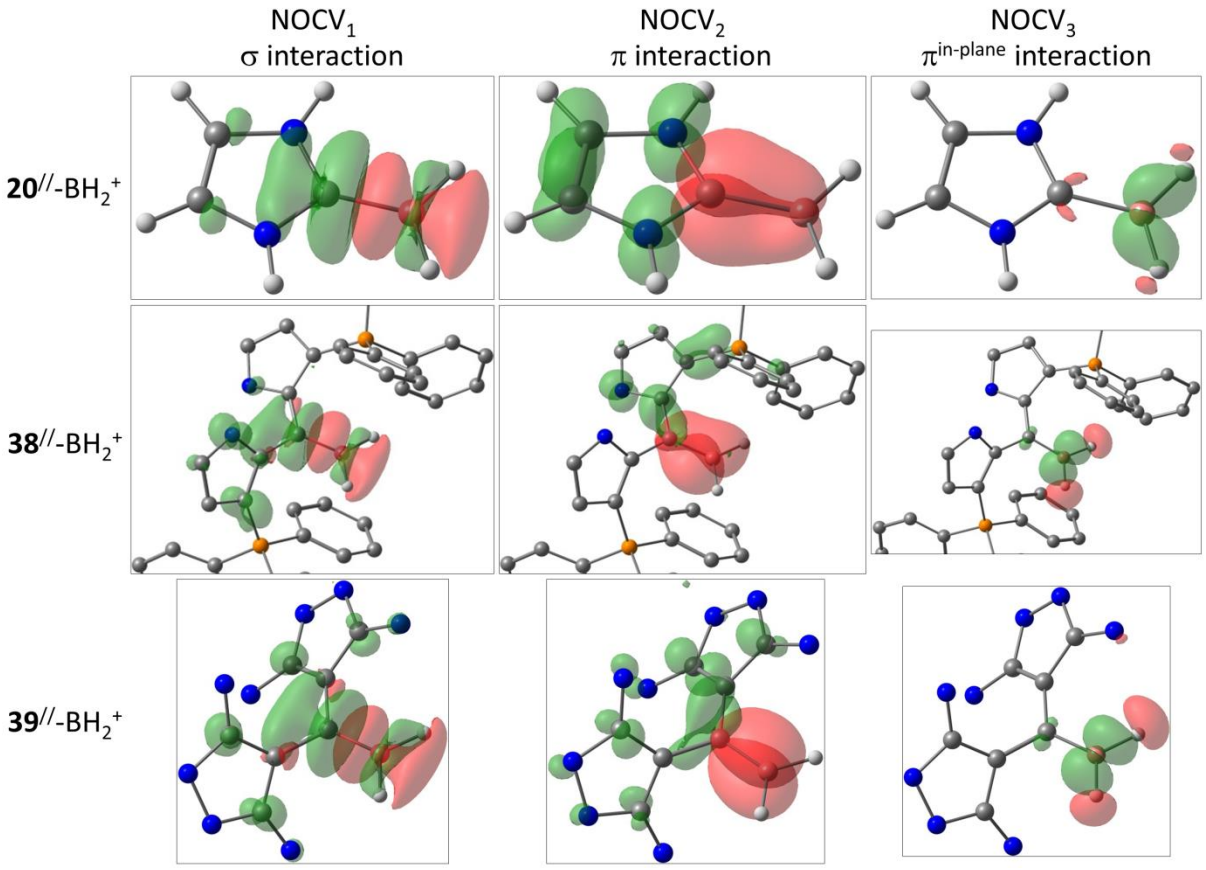

Figure 3. Deformation densities associated with the orbital interactions in $\mathbf{X}^{//}$-BH_2^+ (**X** = **20**, **38** and **39**). The charge flow of the electronic density is green → red. For **X**=**38** and **39**, H atoms, except BH_2, have been omitted for clarity. Isosurface value: 0.003 a.u.

All $\mathbf{X}^{//}$-BH_2^+ complexes showed similar features regarding the description of the bonding between C-donor and borenium within $\mathbf{X}^{//}$-BH_2^+. Three main contributions accounting for about 90% of the total orbital interaction (Table S4) can be identified in the deformation density (Figure 3). The first pair of NOCV, $NOCV_1$, is the strongest contribution. It corresponds to a σ-type interaction which can be described as the $\mathbf{X}\rightarrow BH_2^+$ σ-donation. The second deformation density $NOCV_2$ displays a π-type interaction: the π charge flow from the C-donor ligand to the vacant p orbital of the boron atom suggests that it corresponds to the π-donation. The third contribution $NOCV_3$ corresponds to a π-type interaction located in the Y_2C-BH_2 plane.

Surprisingly, neither the flow of electron density associated with the π-donation, $\Delta q^{//}_{\pi} = \upsilon^{//}_2$, nor the energy associated with the π-donation interaction, $\Delta E^{//}_{\pi} = \Delta E^{//}_2$, provide a very good correlation with $pop(^{//}p_{vac}{}^{B})$ or $E^{//}_{del}$, respectively (Figures 4A and S4). Do these non-perfect correlations illustrate a disagreement between the NBO and ETS-NOCV methods? It should be noted that the π-type interaction corresponding to the second deformation density has been shown to include not only the contribution of the π-donation but also the π-polarization of the C-donor fragment, i.e. the reorganization of π-electron density inside **X** due to the formation of the σ-bond.[95] Thus, the previous non-satisfactory correlations could also be explained by a misinterpretation of the ETS-

NOCV results. To investigate this hypothesis, the ETS-NOCV π-donation energy ($\Delta E^{//}_{\pi}$) calculated for **X**$^{//}$-BH_2^+ complexes by deduction from $\Delta E^{//}_{\pi}$ has been adjusted. The corrected ETS-NOCV π-donation energy ($\Delta E^{//}_{\pi\,corr}$) is obtained by deduction of the π-contribution calculated by the same approach for **X**-H^+ complexes from $\Delta E^{//}_{\pi}$ (Table S5 and Figure S5).[95] Satisfyingly, a much better linear correlation is obtained between $\Delta E^{//}_{\pi\,corr}$ and $E^{//}_{del}$. The only outlier is the **38**$^{//}$-BH_2^+ complex and by excluding this complex the correlation is excellent (R^2 = 0.99, Figure 4B), which validates the hypothesis and demonstrates that the intrinsic strength of the π-interaction, previously defined from the NBO-based indicators, can also be calculated by the ETS-NOCV method provided that the polarization of the fragments is taken into account. Similarly, a strong quadratic correlation is obtained between pop($^{//}p_{vac}^{B}$) and $\Delta q^{//}_{\pi\,corr} = \upsilon^{//}_2 - \upsilon_2$(**X**-$H^+$) ($R^2$ = 0.99, Figure S4). This confirms our assumption to consider these indicators as reference data for the intrinsic π-bond strength. From a chemical point of view, these results confirm the π-donation capability scale of the divalent C-donor ligands calculated with the NBO method.

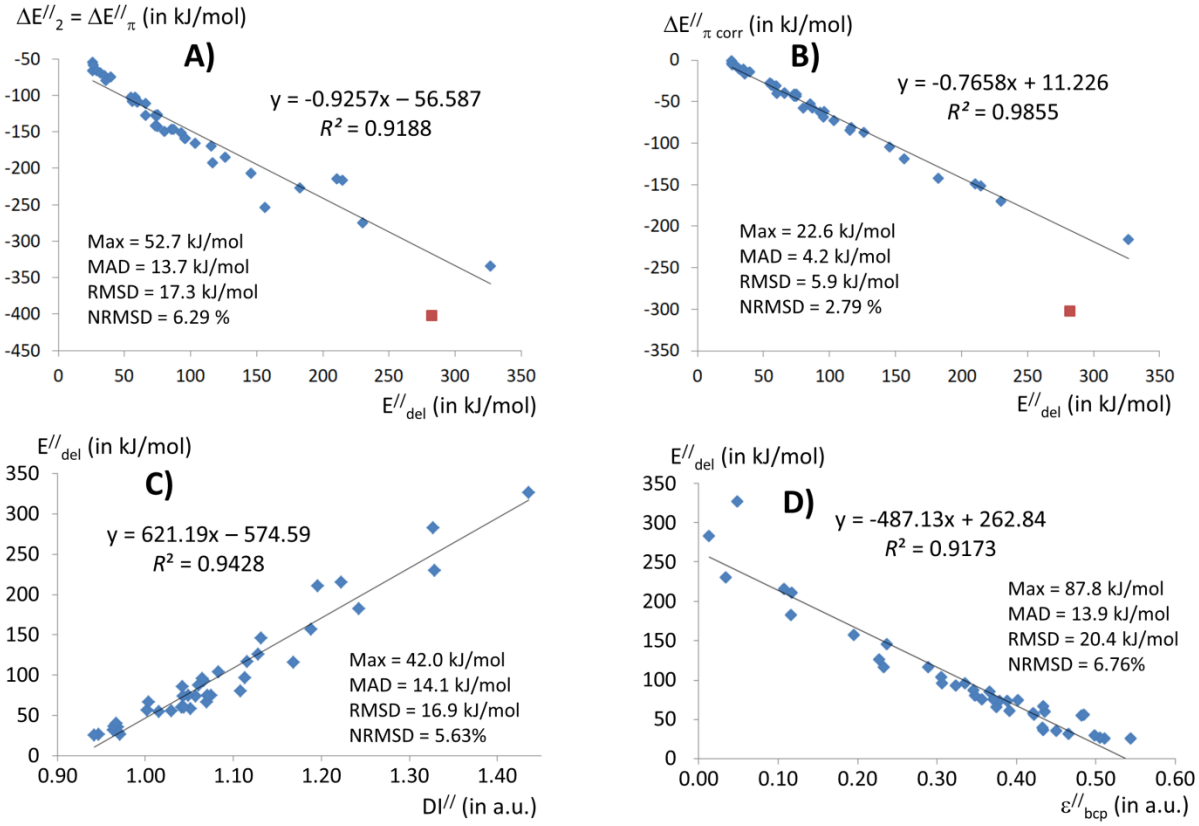

Figure 4. Correlation plots for **X**-BH_2^+ complexes between various descriptors obtained with the NBO and ETS-NOCV (A and B) or QTAIM (C and D) methods. The brown square corresponds to **X** = **38** and is not included in the trendlines for A and B.

Analysis of deformation densities enables to explain the discrepancy observed for complex **38**$^{//}$-BH_2^+ with the ETS-NOCV method. With respect to the bisector plane of the **X**$^{//}$-BH_2^+ complexes, which is perpendicular to the complex plane and goes through the B-C axis, the deformation densities corresponding to the σ- and π-interactions (Figure 3) are symmetrical, in the sense that they involve both moieties of the C-donor ligand in an equivalent manner. This characteristic is observed for all complexes, except **38**$^{//}$-BH_2^+ for which the charge depletion of one moiety of **38** is observed only for $NOCV_1$, whereas the other part is involved only in $NOCV_2$ (Figure 3). Moreover, with respect to the plane defined by the C-BH_2 moiety, the inflow part of the deformation density in $NOCV_2$ for **38**$^{//}$-BH_2^+

is not perfectly symmetrical, contrary to what is observed for all other complexes. These visualizations suggest that $NOCV_1$ and $NOCV_2$ do not fit exactly with purely σ- and π-interactions, respectively, but that σ- and π-interactions are partly combined in these two NOCVs. Thus, the σ-interaction in **38**$^{//}$-BH_2^+ would be underestimated, while the π-interaction would be overestimated, explaining its outlier behaviour.

The same polarization correction approach can be used to estimate the *relative* strength of the π-interaction through the ETS-NOCV method. To that end, the ETS-NOCV $\pi^{\text{in-plane}}$-donation energy ($\Delta E^{\perp}_{\pi\ \text{in-plane}}$) has been calculated for **X**$^{\perp}$-BH_2^+ complexes (Table S6 and Figure S5). Without correction of the polarization, $E^{//}_{del} - E^{\perp}_{del}$ and ΔE_{rot} correlates modestly with $\Delta E^{//}_{\pi} - \Delta E^{\perp}_{\pi\ \text{in-plane}}$ (R^2 = 0.91 and 0.87 respectively, Figure S4). The correlation is improved significantly by applying a polarization correcting on $\Delta E^{//}_{\pi}$ and $\Delta E^{\perp}_{\pi\ \text{in-plane}}$ (R^2 = 0.97 and 0.94, Figure S4). It should be noted, as already mentioned above, that this approach neglects hyperconjugation in both **X**$^{//}$-BH_2^+ ($\pi^{\text{in plane}}$ interaction between σ(B-H) and σ(C-Y) bonds) and **X**$^{\perp}$-BH_2^+ (interaction between the π system of **X** and σ(B-H) bonds) complexes. The intensity of these interactions corrected for polarization has been computed through the ETS-NOCV approach (Tables S4-S6). These interactions are not only relatively lows and roughly similars for all complexes (the maximum value is 36 kJ/mol for **33**$^{\perp}$-BH_2^+) but also they approximately compensate for each other, which justifies this approximation.

Unlike $\Delta E_{del} = E^{//}_{del} - E^{\perp}_{del}$ which is overestimated compared to ΔE_{rot} (*vide supra*), $\Delta E^{//}_{\pi\ corr} - \Delta E^{\perp}_{\pi\ \text{in-plane}\ corr}$ has approximately comparable absolute values compared to ΔE_{rot} (Figure S4). Consequently, the ETS-NOCV absolute energy values, when the polarization of the fragments is taken into account, are more reliable than those obtained by the NBO method. The former should therefore be preferred if reasonable absolute measures of the relative and intrinsic π-bond strengths are requested.

π-bonding descriptors based on the QTAIM approach

The QTAIM method provides a partition of the molecular space into atomic basins. The molecular graph and the electronic density contour map in the molecular plan of **33**$^{//}$-BH_2^+ is depicted in Figure 5A. This method affords the possibility of estimating the π-bond strength using different descriptors, which can be either local or global. Local chemical indexes include the charge density ρ and the ellipticity ε derived from characteristics of the density at the bond critical point (bcp), and the Delocalization Index (DI) corresponds to the global index. It is well known that ρ_{bcp} and DI can be used to estimate the bond order.[104-106] More precisely, a logarithmic relationship was proposed between ρ_{bcp} and the bond order estimated by DI:[105] $DI = \exp[A(\rho_{bcp} - B)]$. At the B3LYP/TZVP level of calculation, the data points for the C-B bond in the 39 **X**$^{//}$-BH_2^+ complexes fit reasonably well to this equation with A = 10.4644, B = 0.1725 and R^2 = 0.92. A quadratic regression slightly improves the correlation with R^2 = 0.94 (Figure S6). Comparison between indexes $\rho^{//}_{bcp}$ or $DI^{//}$ and those previously calculated clearly shows that the delocalization index provides more valuable information. This is reflected in a good linear correlation between $DI^{//}$ and $E^{//}_{del}$ (R^2 = 0.94, Figure 4C). Other measures of the *intrinsic* strength of the π-interaction, such as pop($^{//}p_{vac}^{B}$) and $\Delta E^{//}_{\pi\ corr}$ give similar correlation with respect to $DI^{//}$ (respectively R^2 = 0.95 and 0.94 excluding **38**$^{//}$-BH_2^+, Figure S6). Conversely, other indicators, such as $d_{C\text{-}B}$, $\Delta E^{//}_{\pi}$ or ΔE_{rot} for which a lower performance for estimating the *intrinsic* strength of the π-interaction has been shown above, give lower correlations (R^2 = 0.88, 0.92 and 0.92, respectively, not displayed). Similarly, ΔDI, calculated as the difference between the delocalization indexes $DI^{//}$ and $DI^{\perp}$ computed respectively for **X**$^{//}$-BH_2^+ and **X**$^{\perp}$-BH_2^+, turns out to be a good measure of the *relative* strength of the π-interaction, as revealed by the good correlation between ΔDI and ΔE_{rot} (R^2 = 0.96, Figure S6).

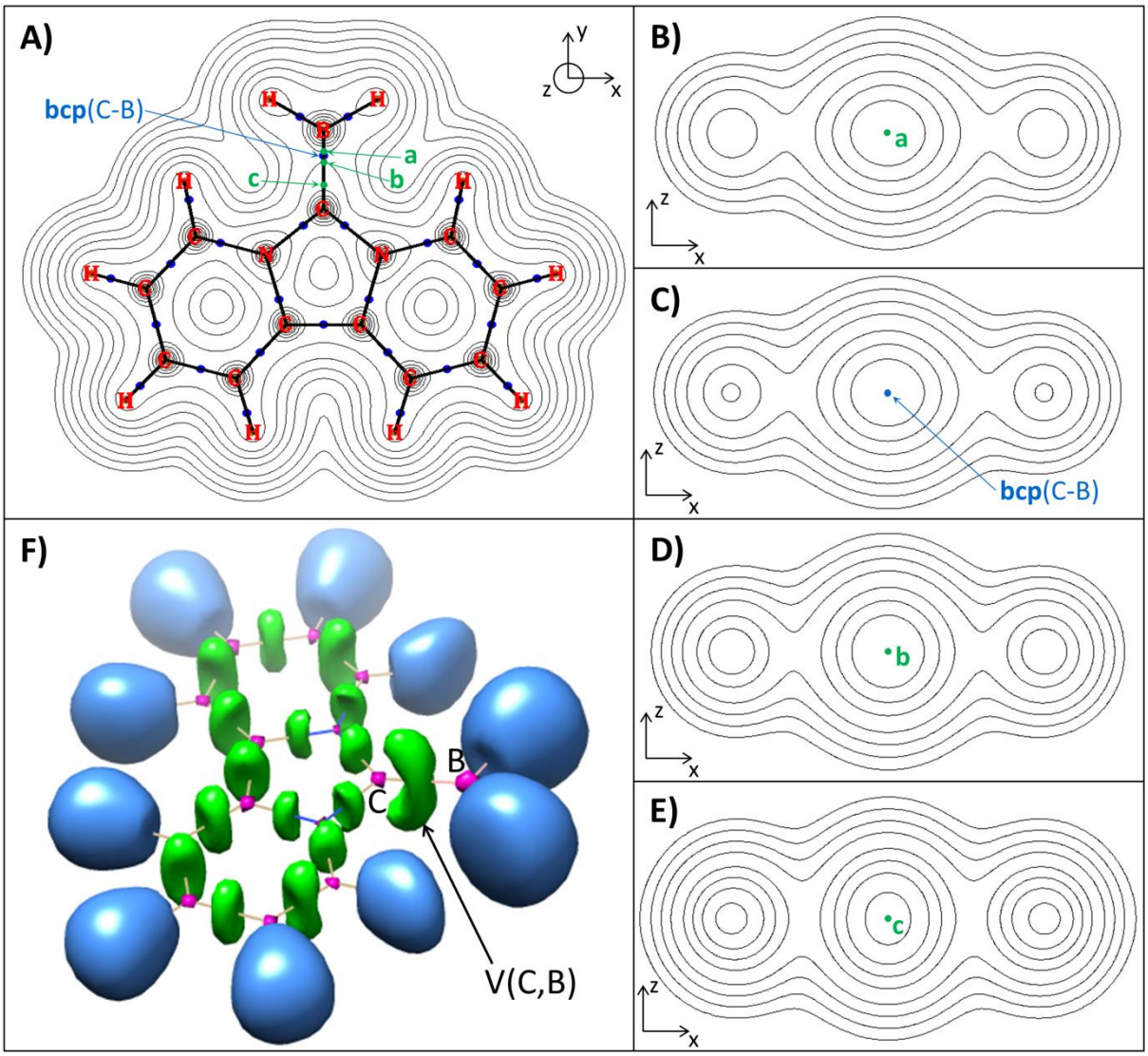

Figure 5. . QTAIM molecular graph (blue points and bold black lines represent bond critical points and bond paths, respectively. The bcp of the C-B bond path is highlighted) and contour map of ρ in the molecular plan of **33**$^{//}$-BH_2^+ (A); contour map of ρ of **33**$^{//}$-BH_2^+ in a xz plane containing the point a corresponding to the largest negative ε_{corr} value along the C-B bond path (B), the carbon-boron bcp (C), the point b of the C-B bond path defined by $\varepsilon_{corr}(b) = 0$ (D) and the point c corresponding to the largest positive ε_{corr} value along the C-B bond path (E) (see Figure S7 for the variation of ε_{corr} along the C-B bond path for **33**$^{//}$-BH_2^+); isosurface (0.80) ELF representation for **33**$^{//}$-BH_2^+ (color code: magenta = core, green = disynaptic valence, light blue = protonated disynaptic).

The ellipticity of the electron density at the bond critical points, ε_{bcp}, is a parameter computed in the framework of the AIM analysis.[107] This parameter provides a quantitative measurement of the anisotropy of the electron density at the bcp. This measure of the deviation of the charge distribution of the bond from axial symmetry is provided by the ratio between the two negative curvatures λ_1 and λ_2 of ρ at the bond critical point: $\varepsilon_{bcp} = \lambda_1 / \lambda_2 - 1$ (with $|\lambda_1| > |\lambda_2|$). Therefore, the ellipticity has been logically associated with the π character of bonds. For a single bond, $\varepsilon_{bcp} = 0$ because $\lambda_1 = \lambda_2$. For double bonds, the decrease of the density in the direction of the π-system should be smaller than that in the σ-plane of the bond. Consequently, the π-direction defines the λ_2 curvature which leads to $\varepsilon_{bcp} > 0$, ε_{bcp} being at maximum for bonds of order 2. On this basis, it seems

satisfactory to obtain a significant linear correlation between ε_{bcp} and $E^{//}_{del}$ (R^2 = 0.92, Figure 4D). This trend is however highly surprising because an ellipticity close to zero is obtained for molecules which possess a large π-interaction whereas molecules with low $E^{//}_{del}$ values show large ε_{bcp} values.

In order to explain this unexpected result, we focus our study on **1**$^{//}$-BH_2^+, **21**$^{//}$-BH_2^+ and **37**$^{//}$-BH_2^+, which respectively show small, medium and large π-interaction. The calculation for these complexes of the ellipticity $\varepsilon(d) = \lambda_1(d) / \lambda_2(d) - 1$ (with $|\lambda_1(d)| > |\lambda_2(d)|$) along the C-B bond, at the distance d from the C atom, reveals two maxima around d = 0.4 and 1.1 Å separated by a minimum value close to zero and located near the middle of the C-B bond (Figure 6). A similar result is obtained for the planar conformation of CH_2-BH_2^+ which possesses a pure σ-CB bond as its π-system is empty. On the other hand, this result differs strongly from what is obtained for the CC double bond in CH_2=CH_2 or the CB double bond in CH_2=BH_2^-, for which a single maximum is calculated along the bond.

These findings are explained by a thorough examination of the negative eigenvalues $\lambda_1(d)$ and $\lambda_2(d)$ ($|\lambda_1(d)| > |\lambda_2(d)|$) of $\Delta\rho(d)$ along the bond. For the sake of clarity, the curvature of $\rho(d)$ along the π direction is named $\lambda_\pi(d)$, while the curvature in the plane of the molecule along the axis perpendicular to the bond is noted $\lambda_{\pi\ in\text{-}plane}(d)$. We also define $\varepsilon_{corr}(d) = \lambda_{\pi\ in\text{-}plane}(d) / \lambda_\pi(d) - 1$. For CH_2=CH_2 and CH_2=BH_2^-, as expected, $\lambda_2(d) = \lambda_\pi(d)$ at the bcp and its neighbourhood, which means that $\varepsilon(d) = \varepsilon_{corr}(d)$ (Figure 6). However, this is not the case close to the bond ends where $\lambda_1(d) = \lambda_\pi(d)$ and $\varepsilon(d) \neq \varepsilon_{corr}(d)$. More precisely, $\varepsilon_{corr}(d)$ turns negative, which is an indication that the decrease of the density is faster in the π-direction than in the plane of the molecule. We assume that this is due to the proximity of the C-H and B-H σ-bond. Similar behaviour is observed for **X**$^{//}$-BH_2^+ complexes as illustrated by the contour map of ρ at various planes perpendicular to the B-C bond (Figures 5B-E and S7). This assumption enables us to explain the 2 maxima of $\varepsilon(d)$ obtained for CH_2-BH_2^+, which do not reflect any π system of the molecule but the presence of the C-H and B-H bonds at both bond ends. As the C-B bond is polarized, due to the low boron electronegativity, the bcp is located approximately at 2/3 of the CB bond, on the boron side, i.e. in the region of greatest influence of the B-H bonds. ε_{bcp} is thus large even if the C-B bond in CH_2-BH_2^+ is not a double bond. The influence of the rising π-donation from **1**$^{//}$-BH_2^+ to **21**$^{//}$-BH_2^+ and **37**$^{//}$-BH_2^+ is thus clearly visible when calculating $\varepsilon_{corr}(d)$ along the B-C axis, with an increasing maximum located on the C atom side. The local character of ε_{bcp} does not allow this feature to be distinguished, and, on the contrary, this descriptor can be misleading because it does not distinguish the direction of the curvatures λ_1 and λ_2. Attempts to use $\varepsilon_{corr}(d)$ as a π-bond descriptor were unsuccessful. With respect to $E^{//}_{del}$, the best correlation, using the maximum of $\varepsilon_{corr}(d)$, gives only a poor correlation with R^2 = 0.79 (Figure S6).

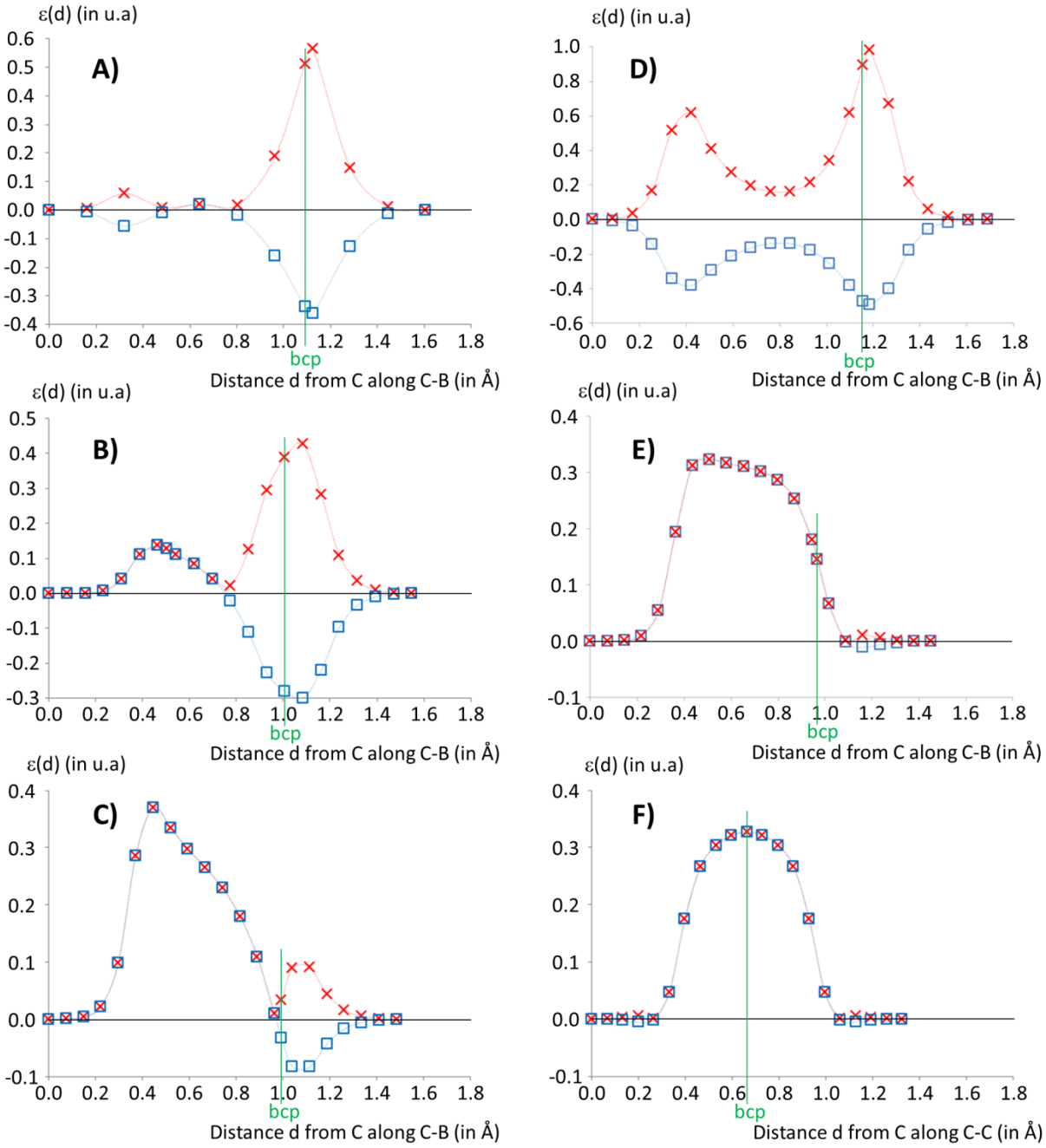

Figure 6. Variation of ellipticity indices $\varepsilon(d) = \lambda_1(d) / \lambda_2(d) - 1$ (with $|\lambda_1(d)| > |\lambda_2(d)|$) (red cross) and $\varepsilon_{corr}(d) = \lambda_{\pi\ in\text{-}plane}(d) / \lambda_{\pi}(d) - 1$ (blue square), calculated at the distance d from the C atom along the C-B or C-C bond for A) $\mathbf{1}^{//}$-BH_2^+, B) $\mathbf{21}^{//}$-BH_2^+, C) $\mathbf{37}^{//}$-BH_2^+, D) $CH_2^{//}$-BH_2^+, E) CH_2=BH_2^- and F) CH_2=CH_2.

π-bonding descriptors based on the ELF approach

The topological analysis of the electron localization function (ELF) provides a partition of the molecular space into core and valence basins (Figure 5F). This method allows the study of chemical bonds as a one-to-one correspondence between the valence basins, and lone pairs or Lewis-type bonds has been achieved.[21] The ELF method was previously used to study the interaction between NHC and main group fragments.[108-110] Integration of the electronic density over the basin corresponding to the C-B bond, V(C,B), is used to calculate the population of the C-B bond in $\mathbf{X}^{//}$-BH_2^+, $pop^{//}[V(C,B)]$. As expected, this population reflects the *intrinsic* π character of the bond, as shown by the correlation with $E^{//}_{del}$. The best fit is obtained with a logarithmic relationship (R^2 = 0.94,

Figure S6). Calculation of the difference in the population of the C-B bond in $\mathbf{X}^{//}$-BH_2^+ and $\mathbf{X}^{\perp}$-BH_2^+, $\Delta pop = pop^{//}[V(C,B)] - pop^{\perp}[V(C,B)]$, gives a much weaker correlation with respect to ΔE_{rot} (R^2 = 0.81, Figure S6), showing that Δpop is not a good descriptor for measuring the *relative* strength of the π-interaction.

Conclusion

In the course of this work, the comparison between five modeling approaches based on DFT calculations (Optimized structure, NBO, ETS-NOCV, QTAIM and ELF) for estimating the magnitude of the π-donation has been achieved. Chemical systems, combining various divalent C-donor ligands with a BH_2^+ borenium group, have been designed. They include a partial CB π-bond resulting from a π-donation that is not biased by any other π-interaction between the two fragments and toward the boron atom. The intensity of the π-bond has been estimated from a wide selection of indicators and compared with each other. The different modelling methods enable the calculation of π-bond descriptors which correlate very well with each other (R^2 between 0.94 and 0.99) and therefore appear to describe the same chemical property. They thus give a quantitative scale of increasing π-donation ability of **X** ligands from **1** to **39**. This scale indicates that carbodiphosphoranes and carbodicarbenes ligands are the most π-donor compounds while saturated NHC, those including π-withdrawing substituents and cAAC ligands are the weaker π-donors.

Such excellent correlations require adjustments from the standard calculations commonly used in the literature, in particular for ETS-NOCV and QTAIM approaches. The use of these methods without these corrections leads to lower correlations (R^2 < 0.92), or even to disagreements that may suggest that these methods diverge, which is not the case. In detail, the conclusions are as follows:

- A π-bond is characterized by 2 families of indicators: *intrinsic* and *relative* π-bond strength descriptors. Correlations between these two families are moderate (R^2 around 0.90).
- *Intrinsic* indicators describe the intensity of the π-bond in the molecule under study, whereas *relative* indicators measure the difference between the molecule with the π-interaction and the same molecule in a conformation which prevents this interaction.
- The reference *relative* indicator is the rotational barrier around the π-bond ΔE_{rot}. The bond lengths give at best an approximate indication of the strength of the π-bond.
- The NBO method provides three descriptors with moderately good (Wiberg Bond Index WBI) to very good (atomic π-population and NBO energetic analysis through the deletion of selected NBOs) performance to measure the π-bond strength. However, the absolute value of the π-bond energy is systematically overestimated by this approach.
- The π-donation-type NOCV eigenvalue and energy failed to give reliable measure of the π-bond strength. A significantly enhanced accuracy is obtained by correcting the previous values from the polarization of the π-system associated with the π-interaction, showing that NOCV chemical interpretation should be made with caution.
- Although the ETS-NOCV approach does not usually require symmetrical molecules to dissociate σ- and π-contributions, a case has been identified where this method fails and mixes σ- and π-interactions.
- The Delocalization Index (DI) provided by the QTAIM approach reproduces accurately the π-bond strength, contrary to the density value at the bond critical point ρ_{bcp}, which gives less relevant correlations. The ellipticity ε_{bcp} fails drastically for these dative π-bonds, due to the influence of the neighboring σ-bonds which reverse the role of the eigenvalues of the density curvature.

- The bond population given by the ELF method gives a reasonable correlation, but only for the *intrinsic* π-bond strength.

This understanding of the strengths and weaknesses of the calculation methods will help in the appropriate choice of indicators to be used. These chemical and computational insights should enable the design of more π-donor ligands. However, all these correlations have been obtained for a single type of π-interaction between C and B atoms. Further work will be carried out in the future to investigate whether or not these correlations could be extended to other bonds, in particular for the NBO method.

Acknowledgments

This work was performed using HPC resources from GENCI-CINES (Grant A0050806894). R.G. thanks the Ecole Polytechnique for a PhD stipend. G.H. thanks the vice-presidency for marketing and international relations in Ecole Polytechnique for support from the international internship program.

Supporting Information

Computational methods, descriptor's numerical values, correlation plots, deformation densities, electronic energies and Cartesian coordinates

Notes

The authors declare no competing financial interest.

References

[1] J.F. Gonthier, S.N. Steinmann, M.D. Wodrich, C. Corminboeuf, *Chem. Soc. Rev.* **2012**, *41*, 4671-4687.

[2] J. Grunenberg, *Int. J. Quantum Chem.* **2017**, *117*, e25359

[3] L. Pauling, *The nature of the Chemical Bond*. Cornell Univ. Press, **1960**.

[4] L. Zhao, W.H. Schwarz, G. Frenking, *Nat. Chem. Rev.* **2019**, *3*, 35-47.

[5] W. Gordy, *J. Chem. Phys.* **1947**, *15*, 305-310.

[6] P. Pyykkö, M. Atsumi, *Chem. Eur. J.* **2009**, *15*, 12770-12779.

[7] L. Zhao, S. Pan, N. Holzmann, P. Schwerdtfeger, G. Frenking, *Chem. Rev.* **2019**, *119*, 8781-8845.

[8] C.A. Coulson, *Proc. R. Soc. London, Ser. A* **1939**, *169*, 413-428.

[9] K.B. Wiberg, *Tetrahedron* **1968**, *24*, 1083-1096.

[10] I. Mayer, *Chem. Phys. Lett.* **1983**, *97*, 270-274.

[11] I. Mayer, *J. Comput. Chem.* **2007**, *28*, 204-221.

[12] S.F. Boys, *Rev. Mod. Phys.* **1960**, *32*, 296-299.

[13] J. Pipek, P.G. Mezey, *J. Chem. Phys.* **1989**, *90*, 4916-4926.

[14] C. Edmiston, K. Ruedenberg, *Rev. Mod. Phys.* **1963**, *35*, 457-465.

[15] P.O. Löwdin, *Phys. Rev.* **1955**, *97*, 1474-1489.

[16] Y.M. Rhee, M. Head-Gordon, *J. Am. Chem. Soc.* **2008**, *130*, 3878-3887.

[17] A.J.W. Thom, E.J. Sundstrom, M. Head-Gordon, *Phys. Chem. Chem. Phys.* **2009**, *11*, 11297-11304.

[18] E.D. Glendening, C.R. Landis, F. Weinhold, *WIREs Comput. Mol. Sci*. **2012**, *2*, 1-42.

[19] R.F.W. Bader, *Atoms in molecules: A quantum theory*. Oxford Univ. Press, **1990**.

[20] A.D. Becke, K.E. Edgecombe, *J. Chem. Phys.* **1990**, *92*, 5397-5403.

[21] B. Silvi, A. Savin, *Nature* **1994**, *371*, 683-686.

[22] E.R. Johnson, S. Keinan, P. Mori-Sanchez, J. Contreras-Garcia, A.J. Cohen, W.J. Yang, *Am. Chem. Soc.* **2010**, *132*, 6498-6506.

[23] P. de Silva, C. Corminboeuf, *J. Chem. Theory Comput.* **2014**, *10*, 3745-3756.

[24] P.B. Karadakov, K.E. Horner, *J. Chem. Theory Comput.* **2016**, *12*, 558-563.

[25] G. Bistoni, L. Belpassi, F. Tarantelli, *J. Chem. Theory Comput.* **2016**, *12*, 1236–1244.

[26] B. Jeziorski, R. Moszynski, K. Szalewicz, *Chem. Rev.* **1994**, *94*, 1887-1930.

[27] T. Ziegler, A. Rauk, *Inorg. Chem.* **1979**, *18*, 1558-1565.

[28] T. Ziegler, A. Rauk, *Inorg. Chem.* **1979**, *18*, 1755-1759.

[29] K. Morokuma, *J. Chem. Phys.* **1971**, *55*, 1236-1244.

[30] M.P. Mitoraj, A. Michalak, T. Ziegler, *J. Chem. Theory Comput.* **2009**, *5*, 962-975.

[31] M. Kaupp, D. Danovich, S. Shaik, *Coord. Chem. Rev.* **2017**, *344*, 355-362.

[32] E. Kraka, D. Cremer, *ChemPhysChem* **2009**, *10*, 686-698.

[33] D. Setiawan, R. Kalescky, E. Kraka, D. Cremer, *Inorg. Chem.* **2016**, *55*, 2332-2344.

[34] K. Brandhorst, J. Grunenberg, *Chem. Soc. Rev.* **2008**, *37*, 1558-1567.

[35] L. Zhao, M. Hermann, W.H.E. Schwarz, G. Frenking, *Nat. Rev. Chem.* **2019**, *3*, 48-63.

[36] L. Pecher, R. Tonner, *WIREs Comput. Mol. Sci.* **2019**, *9*, e1401.

[37] L. Zhao, M. von Hopffgarten, D.M. Andrada, G. Frenking, *WIREs Comput. Mol. Sci.* **2018**, *8*, e1345.

[38] C. Lepetit, P. Fau, K. Fajerwerg, M.L. Kahn, B. Silvi, *Coord. Chem. Rev*. **2017**, *345*, 150-181.

[39] F. Weinhold, C.R. Landis, E.D. Glendening, *Int. Rev. Phys. Chem.* **2016**, *35*, 399-440.

[40] J.P. Dognon, *Coord. Chem. Rev.* **2014**, 266-267, 110-122.

[41] E. Matito, M. Sola, *Coord. Chem. Rev.* **2009**, *253*, 647-665.

[42] R.F.W. Bader, *Chem. Rev.* **1991**, *91*, 893-928.

[43] S. Dutta, B. Maity, D. Thirumalai, D. Koley, *Inorg. Chem.* **2018**, *57*, 3993-4008.

[44] F. Cortes-Guzman, R.F.W. Bader, *Coord. Chem. Rev.* **2005**, *249*, 633-662.

[45] M. Fugel, J. Beckmann, D. Jayatilaka, G.V. Gibbs, S. Grabowsky, *Chem. Eur. J.* **2018**, *24*, 6248-6261.

[46] M. Fugel, M.F. Hesse, R. Pal, J. Beckmann, D. Jayatilaka, M.J. Turner, A. Karton, P. Bultinck, G.S. Chandler, S. Grabowsky, *Chem. Eur. J.* **2018**, *24*, 15275-15286.

[47] X. Wu, L. Zhao, J. Jin, S. Pan, W. Li, X. Jin, G. Wang, M. Zhou, G. Frenking, *Science*, **2018**, *361*, 912-916.

[48] C.R. Landis, R.P. Hughes, F. Weinhold, *Science*, **2019**, *365*, 10.1126/science.aay2355.

[49] L. Zhao, S. Pan, M. Zhou, G. Frenking, *Science*, **2019**, *365*, 10.1126/science.aay5021.

[50] C.R. Landis, R.P. Hughes, F. Weinhold, *Organometallics*, **2015**, *34*, 3442–3449

[51] P. Jerabek, H.W. Roesky, G. Bertrand, G. Frenking, *J. Am. Chem. Soc.* **2014**, *136*, 17123-17135.

[52] J. Molina Molina, J.A. Dobado, G.L. Heard, R.F.W. Bader, M.R. Sundberg, *Theor. Chem. Acc.* **2001**, *105*, 365-373.

[53] Y. Xie, R.S. Grev, J. Gu, H.F. Schaefer III, P.v.R. Schleyer, J. Su, X.W. Li, G.H. Robinson, *J. Am. Chem. Soc.* **1998**, *120*, 3773-3780.

[54] K.W. Klinkhammer, *Angew. Chem. Int. Ed. Engl.* **1997**, *36*, 2320-2322.

[55] F. Weinhold, R.A. Klein, *Angew. Chem. Int. Ed.* **2015**, *54*, 2600-2602.

[56] G. Frenking, G.F. Caramori, *Angew. Chem. Int. Ed.* **2015**, *54*, 2596-2599.

[57] F. Weinhold, R.A. Klein, *Angew. Chem. Int. Ed.* **2014**, *53*, 11214-11217.

[58] A.J. Stone, K. Szalewicz, *J. Phys. Chem. A* **2018**, *122*, 733-736.

[59] F. Weinhold, E.D. Glendening, *J. Phys. Chem. A* **2018**, *122*, 724-732.

[60] A.J. Stone, *J. Phys. Chem. A* **2017**, *121*, 1531-1534.

[61] F. Weinhold, P.v.R. Schleyer, W.C. McKee, *J. Comput. Chem.* **2014**, *35*, 1499-1508.

[62] F.M. Bickelhaupt, E.J. Baerends, *Angew. Chem. Int. Ed.* **2003**, *42*, 4183-4188.

[63] F. Weinhold, *Angew. Chem. Int. Ed.* **2003**, *42*, 4188-4194.

[64] D.M. Andrada, N. Holzmann, T. Hamadi, G. Frenking, *Beilstein J. Org. Chem.* **2015**, *11*, 2727-2736.

[65] P.L. Ayers, R.J. Boyd, P. Bultinck, M. Caffarel, R. Carbo-Dorca, M. Causa, J. Cioslowski, J. Contreras-Garcia, D.L. Cooper, P. Coppens, C. Gatti, S. Grabowsky, P. Lazzeretti, P. Macchi, A. Martin Pendas, P.L.A. Popelier, K. Ruedenberg, H. Rzepa, A. Savin, A. Sax, W.H.E. Schwarz, S. Shahbazian, B. Silvi, M. Sola, V. Tsirelson, *Comput. Theor. Chem.* **2015**, *1053*, 2-16.

[66] J. Andrés, P.W. Ayers, R.A. Boto, R. Carbo-Dorca, H. Chermette, J. Cioslowski, J. Contreras-Garcia, D.L. Cooper, G. Frenking, C. Gatti, F. Heidar-Zadeh, L. Joubert, A. Martin Pendas, E. Matito, I. Mayer, A.J. Misquitta, Y. Mo, J. Pilmé, P.L.A. Popelier, M. Rahm, E. Ramos-Cordobo, P. Salvador, W.H.E. Schwarz, S. Shahbazian, B. Silvi, M. Sola, K. Szalewicz, V. Tognetti, F. Weinhold, E.L. Zinc, *J. Comput. Chem.* **2019**, *40*, 2248-2283.

[67] F. Weinhold, *J. Comput. Chem.* **2012**, *33*, 2363-2379.

[68] F. Weinhold, *J. Comput. Chem.* **2012**, *33*, 2440-2449.

[69] M. Sola, *Front. Chem.* **2017**, *5*, 22.

[70] M. Sola, *WIREs Comput. Mol. Sci.* **2019**, *9*, e1404.

[71] W.E. Piers, S.C. Bourke, K.D. Conroy, *Angew. Chem. Int. Ed.* **2005**, *44*, 5016-5036.

[72] J.M. Farrell, J.A. Hatnean, D.W. Stephan, *J. Am. Chem. Soc.* **2012**, *134*, 15728-15731.

[73] T.S. De Vries, A. Prokofjevs, E. Vedejs, *Chem. Rev.* **2012**, *112*, 4246-4282.

[74] P. Eisenberger, C.M. Crudden, *Dalton. Trans.* **2017**, *46*, 4874-4887.

[75] B. Rao, K. Kinjo, *Chem. Asian J.* **2018**, *13*, 1279-1292.

[76] M.J. Ingleson, *Top. Organomet. Chem.* **2015**, *49*, 39-71.

[77] D. Franz, S. Inoue, *Chem. Eur. J.* **2019**, *25*, 2898-2926.

[78] M. Fustier-Boutignon, N. Nebra, N. Mézailles, *Chem. Rev.* **2019**, *119*, 8555-8700.

[79] J.E. Radcliffe, J.J. Dunsford, J. Cid, V. Fasano, M.J. Ingleson, *Organometallics*, **2017**, *36*, 4952-4960.

[80] T. Matsumoto, F. Gabbaï, *Organometallics* **2009**, *28*, 4252-4253.

[81] D. McArthur, C.P. Butts, D.M. Lindsay, *Chem. Commun.* **2011**, *47*, 6650-6652.

[82] H.B. Mansaray, A.D.L. Rowe, N. Phillips, J. Niemeyer, M. Kelly, D.A. Addy, J.I. Bates, S. Aldridge, *Chem. Commun.* **2011**, *47*, 12295-12297.

[83] A. Prokofjevs, A. Boussonière, L. Li, H. Bonin, E. Lacôte, D.P. Curran, E. Vedejs, *J. Am. Chem. Soc.* **2012**, *134*, 12281-12288.

[84] M.Q.Y. Tay, B. Murugesapandian, Y. Lu, R. Ganguly, K. Rei, D. Vidovic, *Dalton Trans.* **2014**, *43*, 15313-15316.

[85] J.M. Farrell, D. Schmidt, V. Grande, F. Würthner, *Angew. Chem. Int. Ed.* **2017**, *56*, 11846-11850.

[86] P. Eisenberger, B.P. Bestvater, E.C. Keske, C.M. Crudden, *Angew. Chem. Int. Ed.* **2015**, *54*, 2467-2471.

[87] J.E. Münzer, P. Ona-Burgos, F.M. Arrabal-Campos, B. Neumüller, R. Tonner, I. Fernandez, I. Kuzu, *Eur. J. Inorg. Chem.* **2016**, 3852-3858.

[88] B. Inés, M. Patil, J. Carreras, R. Goddard, W. Thiel, M. Alcarazo, *Angew. Chem. Int. Ed.* **2011**, *50*, 8400-8403.

[89] M. Lafage, A. Pujol, N. Saffon-Merceron, N. Mézailles, *ACS Catal.* **2016**, *6*, 3030-3035.

[90] M.A. Celik, G. Frenking, B. Neumüller, W. Petz, *ChemPlusChem* **2013**, *78*, 1024-1032.

[91] G. Frenking, M. Hermann, D.M. Andrada, N. Holzmann, *Chem. Soc. Rev.* **2016**, *45*, 1129-1144.

[92] N.T.A. Nhung, H.T.P. Loan, P.T. Son, H.V. Duc, D.T. Quang, P.V. Tat, D.T. Hlep, *Theor. Chem. Acc*. **2019**, *138*, 67.

[93] K. Sato, T. Tsai Yuan Tan, F. Schäfers, F.E. Hahn, D.W. Stephan, *Dalton. Trans.* **2017**, *46*, 16404-16407.

[94] H.C. Tsai, Y.F. Lin, W.C. Liu, G.H. Lee, S.M. Peng, C.W. Chiu, *Organometallics*, **2017**, *36*, 3879-3882.

[95] E. Rezabal, G. Frison, *J. Comput. Chem.* **2015**, *36*, 564-572.

[96] H.V. Huynh, G. Frison, *J. Org. Chem.* **2013**, *78*, 328-338.

[97] J.C. Bernhammer, G. Frison, H.V. Huynh, *Chem. Eur. J.* **2013**, *19*, 12892-12905.

[98] H.V. Huynh, *Chem. Rev.* **2018**, *118*, 9457-9492.

[99] D. Munz, *Organometallics* **2018**, *37*, 275-289.

[100] The largest deviation is observed for **8**-BH_2^+ with Y-C-B-H dihedral angle of 13.8°, due to the non-planarity of the NHC moiety.

[101] WBI values have also been calculated for **X**-BH_3 complexes, and the use of these values leads to similar analyses to the ones obtained with WBI(**X**$^{\perp}$-BH_2^+).

[102] M.Q.Y. Tay, G. Ilic, U. Werner-Zwanziger, Y. Lu, R. Ganguly, L. Ricard, G. Frison, D. Carmichael, D. Vidovic, *Organometallics* **2016**, *35*, 439-449.

[103] A.Y. Rogachev, R. Hoffmann, *Inorg. Chem.* **2013**, *52*, 7161-7171.

[104] R.F.W. Bader, T.H. Tang, Y. Tal, F.W. Biegler-König, *J. Am. Chem. Soc.* **1982**, *104*, 946-952.

[105] C.F. Matta, J. Hernandez-Trujillo, *J. Phys. Chem. A* **2003**, *107*, 7496-7504.

[106] C. Outeiral, M.A. Vincent, A. Martin Pendas, P.L.A. Popelier, *Chem. Sci.* **2018**, *9*, 5517-5529.

[107] R.F.W. Bader, T.S. Slee, D. Cremer, E. Kraka, *J. Am. Chem. Soc.* **1983**, *105*, 5061-5068.

[108] G. Frison, A. Sevin, *J. Phys. Chem. A* **1999**, *103*, 10998-11003.

[109] G. Frison, A. Sevin, *J. Organomet. Chem*. **2002**, *643-644*, 105-111.

[110] G. Frison, A. Sevin, *J. Chem. Soc., Perkin Trans. 2* **2002**, 1692-1697.

TOC Graphic

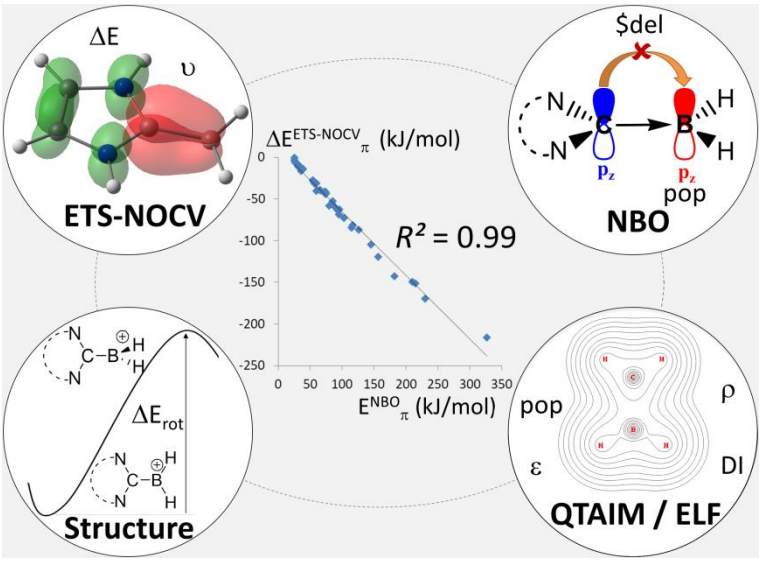

π-bond quantification: Using relevant molecular descriptors is the key to describe the electronic structure. Their comparison was conducted for the π_{CB}-bond of carbene-borenium complexes, revealing the carbene π-donating capability and the strengths and weaknesses of the NBO, ETS-NOCV, QTAIM and ELF methods.

Keywords: Bond energy; Bond theory; Carbene ligands; Computational chemistry; Pi interactions